Hindawi
Journal of Sensors
Volume 2022, Article ID 3590973, 17 pages
https://doi.org/10.1155/2022/3590973

Research Article

Detection and Classification of ADHD from EEG Signals Using Tunable Q-Factor Wavelet Transform

R. Catherine Joy,[1] S. Thomas George,[2] A. Albert Rajan,[3] M. S. P. Subathra,[4] N. J. Sairamya,[5] J. Prasanna,[2] Mazin Abed Mohammed,[6] Alaa S. Al-Waisy,[7] Mustafa Musa Jaber,[8,9] and Mohammed Nasser Al-Andoli[10]

[1]*Department of Electronics and Communication Engineering, Karunya Institute of Technology and Sciences, Coimbatore 641114, India*
[2]*Department of Biomedical Engineering, Karunya Institute of Technology and Sciences, Coimbatore 641114, India*
[3]*Department of Electrical and Electronics Engineering, Karunya Institute of Technology and Sciences, Coimbatore 641114, India*
[4]*Department of Robotics Engineering, Karunya Institute of Technology and Sciences, Coimbatore 641114, India*
[5]*Department of Electrical and Computer Engineering, Université du Québec à Trois-Rivières, 3351 Bd des Forges, Trois-Rivières, QC, Canada G8Z 4M3*
[6]*College of Computer Science and Information Technology, University of Anbar, 31001 Ramadi, Anbar, Iraq*
[7]*Computer Technologies Engineering Department, Information Technology College, Imam Ja'afar Al-Sadiq University, Baghdad, Iraq*
[8]*Department of Computer Science, Dijlah University College, Baghdad, Iraq*
[9]*Department of Computer Science, Al-Turath University College, Baghdad, Iraq*
[10]*Computer Science & Information Systems Department, Faculty of Science, Sa'adah University, Sa'adah, Yemen*

Correspondence should be addressed to Mohammed Nasser Al-Andoli; mnalandoli@saada-uni.edu.ye

Received 12 July 2022; Accepted 2 September 2022; Published 15 September 2022

Academic Editor: Mohit Mittal

The automatic identification of Attention Deficit Hyperactivity Disorder (ADHD) is essential for developing ADHD diagnosis tools that assist healthcare professionals. Recently, there has been a lot of interest in ADHD detection from EEG signals because it seemed to be a rapid method for identifying and treating this disorder. This paper proposes a technique for detecting ADHD from EEG signals with the nonlinear features extracted using tunable Q-wavelet transform (TQWT). The 16 channels of EEG signal data are decomposed into the optimal amount of time-frequency sub-bands using the TQWT filter banks. The unique feature vectors are evaluated using Katz and Higuchi nonlinear fractal dimension methods at each decomposed levels. An Artificial Neural Network classifier with a 10-fold cross-validation method is found to be an effective classifier for discriminating ADHD and normal subjects. Different performance metrics reveal that the proposed technique could effectively classify the ADHD and normal subjects with the highest accuracy. The statistical analysis showed that the Katz and Higuchi nonlinear feature estimation methods provide potential features that can be classified with high accuracy, sensitivity, and specificity and is suitable for automatic detection of ADHD. The proposed system is capable of accurately distinguishing between ADHD and non-ADHD subjects with a maximum accuracy of 100%.

1. Introduction

Attention Deficit Hyperactivity Disorder (ADHD) is one of the prevailing neuropsychiatric disorders among children, and it frequently persists into adulthood [1, 2]. The word-wide study shows that, about 5-12% of prevalence of ADHD is observed among school-going children, and more manifestation is experienced among male children [3–5]. This

disorder has the subtypes such as predominantly inattentive, predominantly hyperactive-impulsive, and the combined type with the primary symptoms of inattention, impulsivity, and hyperactivity [6–8]. Early detection and identification of this disorder and treating in an early stage will be extremely beneficial to children, parents, and especially community health. Currently, clinical interviews, observations, and ratings from multiple sources such as parents and teachers are used to examine and diagnose ADHD [9–11]. The traditional clinical evaluation procedures are time consuming and are subject to ambiguity. Therefore, there is a great need for objective clinical diagnostic methods from the biological signals that reflect the behaviors of ADHD and its subtypes.

Electroencephalography (EEG) is the record of the electrical activities of a human brain, which can reveal a great deal about physiology and pathology. EEG signals have been employed in the diagnosis of several neurological illnesses by extracting unique features and classifying them with different classifiers in automated detection systems. Neurophysiological disorders such as alcoholism [12], dementia [13, 14], epileptic seizure [15], schizophrenia [16, 17], Parkinson's disease [18, 19], and depressive disorder [20, 21] are some of the areas where EEG signals are employed in automatic detection. The EEG signals of ADHD children are different from that normal child in terms of complex randomness, amplitude, and frequency. Researchers have employed several feature extraction techniques and classifiers to analyse EEG signals in the identification of ADHD [22–25]. Researchers have experimented several machine learning algorithms and nonlinear feature extraction approaches such as entropy estimators and classifiers such as support vector machine (SVM), multilayer perceptron, and k-nearest neighbor (KNN) [26–29] to detect ADHD using EEG data. These techniques suffer from higher computational complexity and lower classification accuracy.

A quantifiable brain reaction that happens as a direct result of a sensory, cognitive, or motor event is known as an event-related potential (ERP). Mueller et al. used ERP features to analyse 75 ADHD and 75 normal children and have classified ADHD and normal subjects with a classification accuracy of 91% [30]. Different authors worked on the ERP and extracted probable features that can help detect ADHD, and classification is done with a multilayer neural network and categorized with an accuracy close to 96.7%. [27, 31–33]. While some authors investigated the application of complex deep learning algorithms to diagnose ADHD from EEG signals, others explored more efficient machine learning methodologies. For most of the ADHD detection, the authors extracted nonlinear features and classified with standard classifiers such as support vector machine (SVM), multilayer perceptron, and KNN [26, 28, 29, 34]. A deep convolutional neural networks and deep learning networks were experimented to diagnose ADHD in adults and children [35–37].

Literature reveals that wavelet transform techniques have higher computational efficiency, and they have the added benefit of being able to distinguish tiny details in a signal. Ahmadlou and Adeli [38] employed a wavelet-synchronization pattern recognition methodology with RBF neural network classifier, to detect ADHD with a maximum accuracy of 95.6%. Sadatnezhad et al. [31] used fractal dimension, AR model, and EEG band power to diagnose ADHD children and achieved a maximum classification of 86.4%. Allahverdy et al. [39] analysed EEG data with the nonlinear features extracted using fractal dimension methods and distinguished ADHD subjects with a classification accuracy of 86%. Ahmadlou and Adeli et al. employed the synchronization likelihood (SL) and fuzzy synchronization likelihood (FSL) frameworks to assess functional connectivity and achieving classification accuracies of 87.5% and 95.6%, respectively, for a synchronization pattern in the theta and delta frequency bands [38, 40]. These wavelets transform methods could not achieve the maximum classification accuracy as they could not dynamically adjust the Q value and had lower reconstruction capabilities. To classify ADHD versus normal subjects, these studies largely used artificial intelligence approaches. Based on the literature, different authors expressed that classification accuracy has to be further improved and the computational complexity has to be reduced. Moreover, challenges prevail in identifying the better feature extraction technique and applying the best classifier algorithm for achieving maximum classification accuracy in ADHD diagnostic methods.

To address these difficulties, the authors have experimented an efficient algorithm using tunable Q-wavelet transform (TQWT) with Katz and Higuchi fractional dimension method, that is lighter in computational complexity and with an ANN classifier that provides a maximum classification accuracy. Children with ADHD are identified by the experts and their EEG signals recorded under eyes-open and eyes-closed states are used for this analysis. Potential features are derived from Katz and Higuchi fractal dimensions, which are estimated from the segmented EEG signal subbands. The features extracted through the fractional dimension techniques are classified using the ANN classifier which is a proven effective classifier. The results show that the suggested method is effective in classifying ADHD and normal subjects EEG signals. The main contributions list can be summarized as follows:

(i) The combination of TQWT with Katz and Higuchi fractional dimension method is proven to be an efficient feature extraction method for ADHD detection

(ii) The potential features extracted with the Katz and Higuchi fractional dimension techniques with an ANN classifier brought out with a maximum classification accuracy of 100%

(iii) As the proposed system is lighter in computation with maximum classification accuracy, it can be a resourceful technique for clinical detection of ADHD from the EEG signals

This work is composed of four major sections. Section 2 presents the Materials and Methods, which include data acquisition and feature extraction methods. Section 3 proposes the Results and Discussion, which includes the

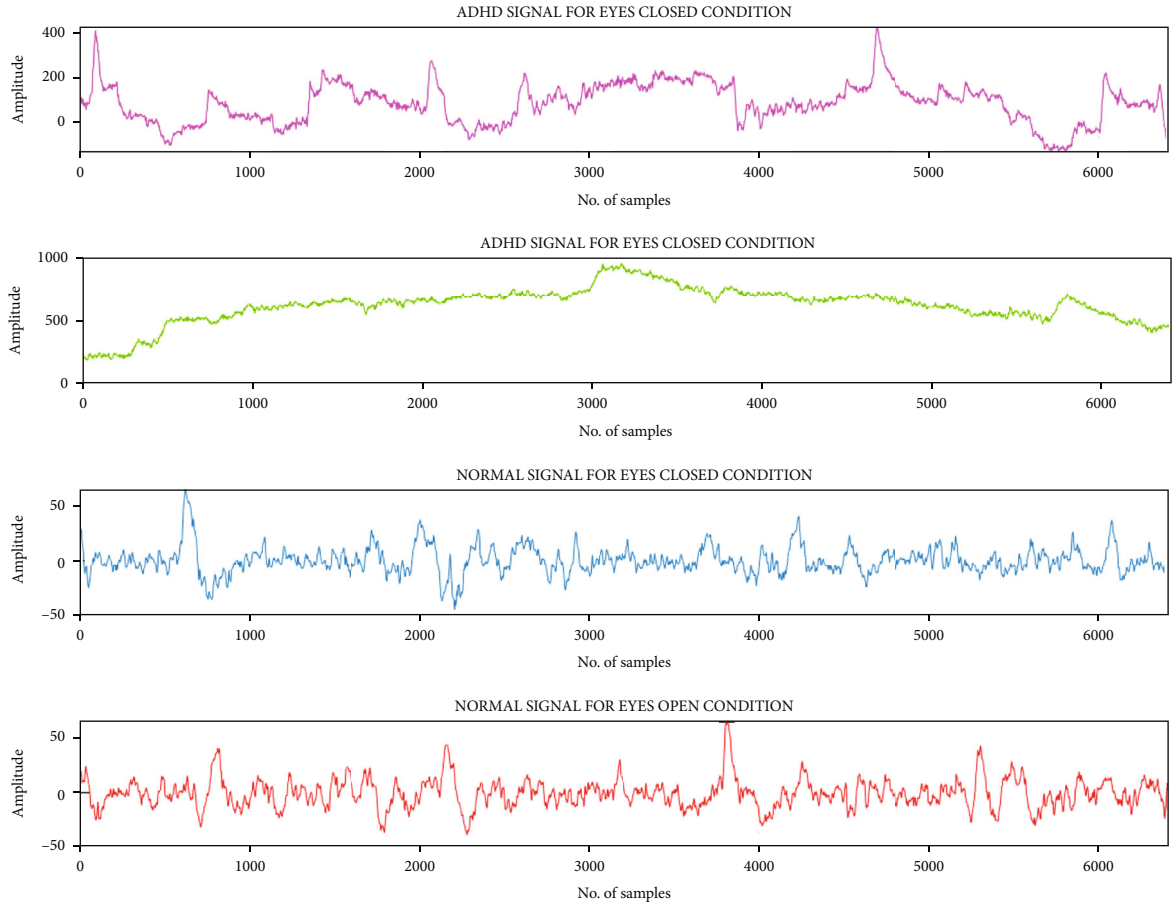

Figure 1: Single-channel EEG signals for ADHD and normal subjects in eyes-closed and eyes-open condition.

analysis of various classifier algorithms, performance metrics, and discussion on comparing similar works. Finally, the Conclusion and future works are presented in Section 4.

2. Materials and Methods

2.1. Data Acquisition. The EEG data set for the proposed approach is created with 5 subjects of ADHD and 5 subjects of normal, in each category under eyes-closed and eyes-open resting state. The EEG signals were recorded from the children age group 7 to 12, after getting parental consent and the children's consent [25]. Using the unipolar setup, the EEG signals of the individuals are measured using the 10–20 electrode placement system. Individual scalps are carefully prepared with a contact impedance of less than $5K\Omega$ for EEG signal measurement. With a sample rate of 256 Hz, each EEG signal consisting of 6400 sampling points was recorded using a 16-electrode unipolar montage. Each signal was captured for 300 seconds with a 24-bit resolution. Signals which acquired are divided into 25 seconds in the eyes-closed resting state and eyes-open resting state in both ADHD and normal subjects. The EEG signals of ADHD and normal subjects are presented in Figure 1.

The acquired signals are preprocessed using MATLAB (MatLabR2018a) to determine the needed range of signals from each channel. Visual inspection and computerized review are carried out with the aid of specialists and a range of signals that are not acceptable for analysis and further processing are removed. A bandpass filter with cutoff frequencies of 1 Hz and 60 Hz is used to reduce signal noise and to eliminate other artefacts and noise during eye blinking. The power frequency noise is suppressed using a 50 Hz notch filter. Experiments are conducted on a laptop with 4 GB of RAM, a 3.2 GHz CPU, and intel core processor. MATLAB 2018a is used to execute the simulations, and the statistical data are recorded for analysing various performance measures. The functional blocks of the proposed methodology for classifying ADHD and normal subjects using the TQWT algorithm is presented in Figure 2.

In this proposed methodology, the EEG signals of both ADHD and normal categories are decomposed into 15 levels of subbands by using TQWT technique. The unique fractal dimension features such as katz and higuchi features are extracted from the decomposed subbands reflecting the ADHD and normal behavior. These features are fed as input to the different classifiers such as linear discriminant, logistic regression, support vector machine, artificial neural networks, and ensemble techniques are experimented to compare the performance of each classifier. The best classifier algorithm with higher classification accuracy is evaluated for choosing the better combination to perform the feature

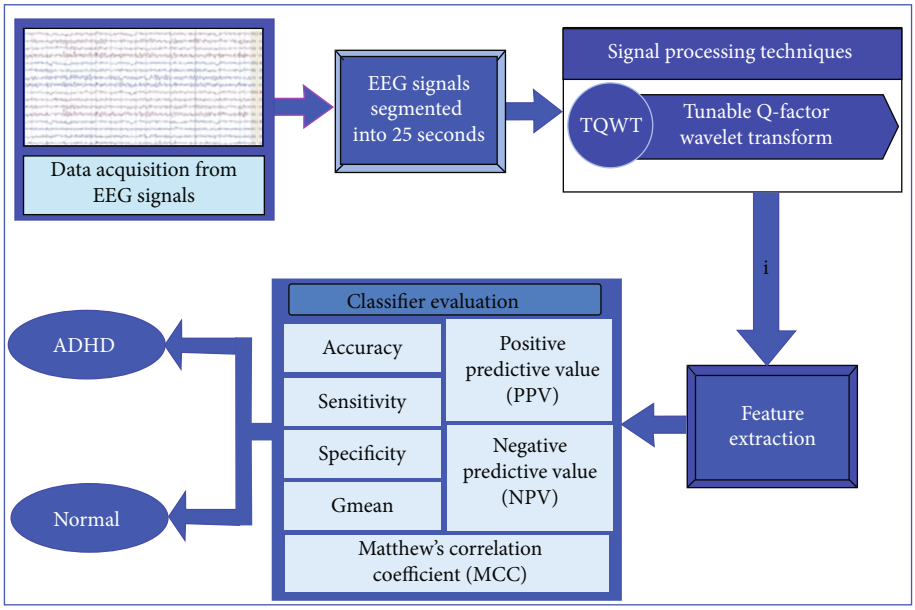

Figure 2: Functional blocks of the proposed methodology.

extraction and classification. The performance of the proposed methodology is verified with different performance metrics for ensuring its best performances.

2.2. Tunable Q-Factor Wavelet Transform (TQWT). The ratio of the centre frequency to the bandwidth of the filters employed in the transform is known as the Q-factor of a wavelet transform. TQWT has the property of fast decomposition and perfect reconstruction which makes it suitable for application in many biomedical signal processing problems. TQWT's efficient decomposition and perfect reconstruction properties make it well-suited to a wide range of biological signal processing applications [41]. The TQWT is a wavelet transform that is analogous to the rational-dilation wavelet transform and has been used to investigate EEG signals [12, 42, 43]. The TQWT provides perfect reconstruction of the signal and the energy of the signal is divided into subbands by the TQWT coefficients. It is done with a discrete wavelet transform that performs a double-channel multirate filter bank with low and high-pass filters. With an adjustable Q-factor and a powerful transform for oscillatory signal analysis, this approach is suited for the discrete-time signal analysis [42]. TQWT's fundamental parameters are its Q-factor (Q), redundancy (r), and the number of levels of decomposition (j) which allow it to analyse signals with a diversity of oscillatory characteristics [44]. TQWT filters are straightforward to reconstruct and implement since they are built up of nonrational transfer functions utilising a Fast Fourier Transform (FFT) with an adjustable Q-factor. In our proposed work, the Q-value factors are modified between 1 and 10, and the classification results are analysed to find the best Q-factor value. The TQWT approach applied to this work is depicted in Figure 3.

Figure 3 shows the different stages of decomposition applied with the TQWT analysis and synthesis filter banks [45]. An EEG signal is divided into j levels by iteratively applying two-channel filter banks on the signal. At each level of decomposition, the input signal $x[n]$ with sampling frequency f_s is decomposed into a high-pass subband signal $x_1[n]$ and a low-pass subband signal $x_0[n]$, with sampling frequencies of αf_s and βf_s, respectively. Here α and β refer scaling factors for the filter banks. Selesnick [42] elaborated a comprehensive description of scaling parameters and proposed that the scaling parameters must fulfil the following criteria to limit redundancy while ensuring perfect reconstruction.

$$\begin{aligned} 0 < \beta \le 1, \\ 0 < \alpha < 1, \\ \alpha + \beta = 1. \end{aligned} \tag{1}$$

The characteristic equation of TQWT can be represented as follows:

$$H_0(\omega) = \begin{cases} 1, |\omega| \le (1-\beta)\,\pi \\ \theta\left(\dfrac{\omega + (\beta-1)\pi}{\alpha+\beta-1}\right), (1-\beta)\pi \le |\omega| < \propto \pi, \\ 0, \alpha\pi \le |\omega| \le \pi \end{cases} \tag{2}$$

$$H_1(\omega) = \begin{cases} 0, |\omega| \le (1-\beta)\,\pi \\ \theta\left(\dfrac{\alpha\pi - \omega}{\alpha+\beta-1}\right), (1-\beta)\pi \le |\omega| < \alpha\pi, \\ 1, \alpha\pi \le |\omega| \le \pi \end{cases} \tag{3}$$

$$\theta(\omega) = \frac{1}{2}\,(1 + \cos\omega)\sqrt{2 - \cos\omega} \text{ for } |\omega| \le \pi. \tag{4}$$

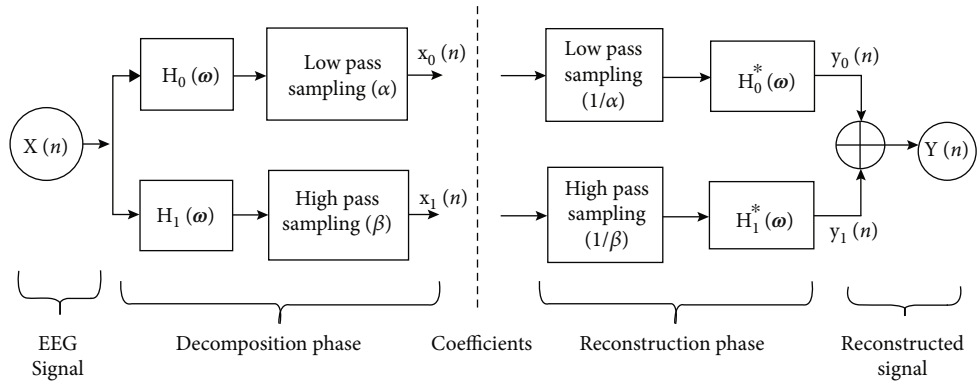

Figure 3: Flow diagram of TQWT analysis and synthesis filter banks.

The bands of $H_0(\omega)$ and $H_1(\omega)$ are constructed using transition function $\theta(\omega)$, which is derived from the Daubechies filter with two vanishing moments. To accomplish the perfect reconstruction criteria, the low-pass filter $H_0(\omega)$ and high-pass filter $H_1(\omega)$ can be assessed using the relation given in equation (2).

$$|H_0(\omega)|^2 + |H_1(\omega)|^2 = 1. \tag{5}$$

The decomposed EEG signals can be reconstructed with the use of a synthesis filter. The relationship between TQWT input parameters and scaling parameters α and β is related by;

$$r = \frac{\beta}{1-\alpha}, \tag{6}$$

$$Q = \frac{2-\beta}{\beta}. \tag{7}$$

The criterion of dominant frequency is used to select the appropriate value of decomposition levels (j). According to the dominant frequency criterion, the number of decomposition levels is kept in such a way that the decomposed subbands have the greatest correlation with substantial EEG frequency ranges.

In this paper, the following feature vectors are evaluated and analysed:

(a) *Q-factor*. The value of Q in TQWT determines the oscillatory behaviour of the signals. EEG signals, in particular, are highly oscillatory in nature and have a high Q-value. The theoretical definition of the Q-factor is expressed as $Q = (2-\beta)/\beta$ and $\alpha = 1 - (\beta/r)$. Based on the values of Q and r, the values of α and β are computed. The value of the Q-factor can be chosen based on the input signal behaviour because it reflects the oscillatory behaviour of the wavelet. If the proposed Q-value is compatible with the input signal's features, it can accurately extract useful information from the EEG signal.

(b) *The maximum number of levels* $j_{\max}$. The scaling parameters α and β, the number of samples (N) in the input signal are used to calculate $j_{\max}$, The maximum levels of decomposition,

$$j_{\max} = \frac{\log(\beta N/8)}{\log(1/\alpha)} \tag{8}$$

(c) *Oversampling rate/redundancy parameter (r)*. The resonance is controlled by the redundancy factor r, which allows the wavelet to be focused in time without affecting its shape. The oversampling rate is defined as r in this case $r = \beta/(1-\alpha)$. When analysing biological signals, the specific number $r = 3$ has been previously recommended [46]. As a result, throughout this research, the redundancy parameter r is chosen as 3

The wavelet transforms technique shall be applied to signals with little or no oscillatory characteristic with a low Q-factor. Most wavelet transforms, except for the continuous wavelet transform, are unable to adjust their Q-factor. This difficulty is solved by TQWT, which allows the Q-factor to be regulated. Moreover, TQWT has been widely employed to investigate a variety of physiological signals [47–49]. Due to the rational transfer functions, the filters are computationally efficient and hence provide direct representation in the frequency domain. As TQWT is a powerful tool for analysing oscillatory physiological signals with lesser computational complexity, the authors felt to apply this technique for the proposed work.

2.3. Feature Extraction. The EEG signals are complex and highly nonlinear in nature. Because of the nonlinear and intricate behaviour, nonlinear methods are appropriate tools for analysing brain dynamics and behaviours from the EEG signals. The Higuchi and Katz fractional dimension based feature extraction methods are more predominantly used for EEG signal analysis [50, 51]. In our work, the Higuchi and Katz nonlinear feature extraction techniques are used to identify the potential features that can help discriminate ADHD and normal subjects.

2.3.1. Higuchi Fractal Dimension. A fractal dimension is a tool for determining nonperiodic and irregular time series.

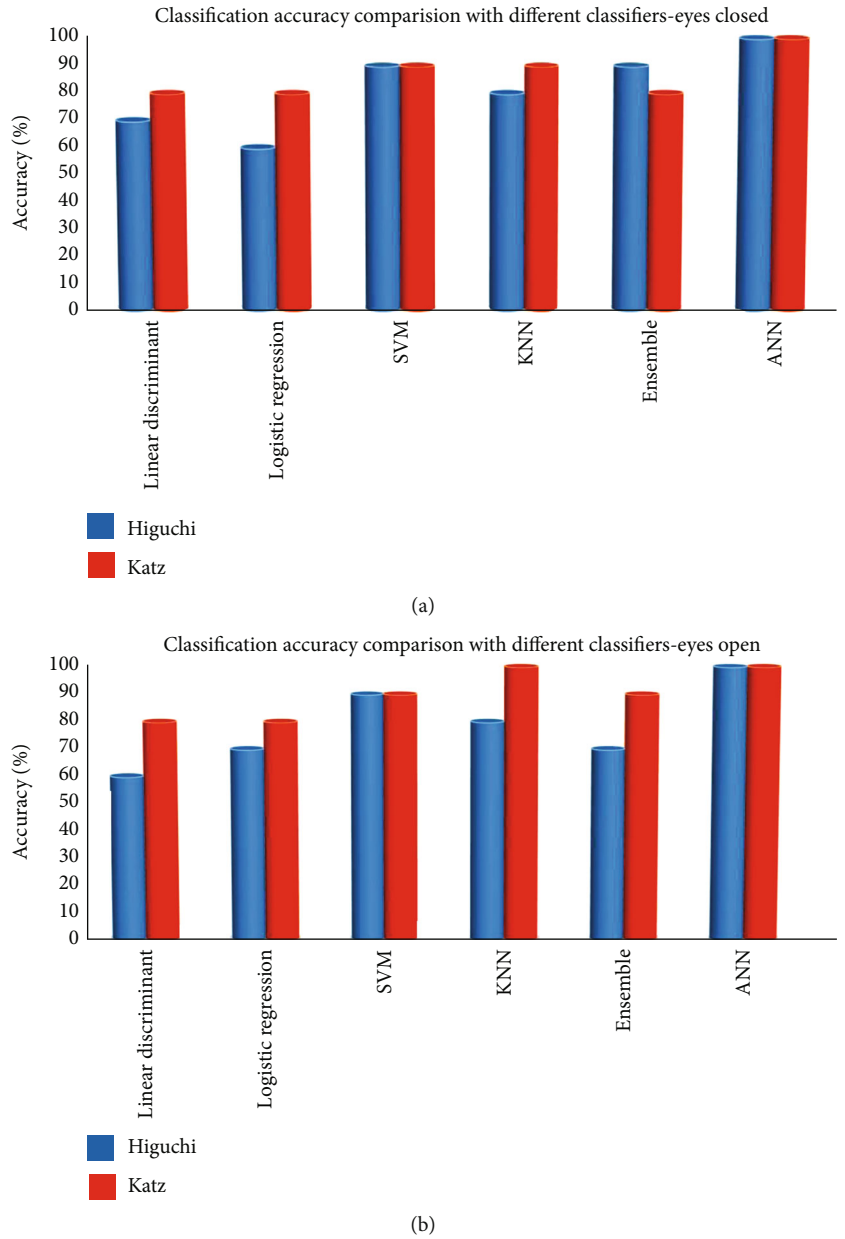

Figure 4: Classification accuracy comparison for different classifiers (a) eyes-closed condition (b) eyes-open condition.

The Higuchi fractional dimension has its high accuracy and efficiency in determining fractal dimensions based on curve length measurements. The time series of the EEG signal is segmented into k number of samples, and the mean length of the series/curve is measured using the segment of k samples [52, 53]. The FD Higuchi estimation can be obtained by following four steps for a finite set of time series, i.e., $S(\tilde{n})$; $\{\tilde{n} = 1, 2, \cdots N\}$; N is the number of points on the curve:

Stage 1. Generate k number of new time series, for values of k ranging from 1 to $k_{\max}$, calculate S_m^k from given time series data.

$$S_m^k = \left\{ S(m), S(m+k), S(m+2k), \cdots, S\left(m + \text{int}\left(\frac{N-m}{k}\right).k \right) \right\}. \tag{9}$$

In this, the discrete time interval between sample points is represented by k, and the initial time value is represented by $m\,(m = 1, 2, 3, \cdots\ldots, k)$.

Stage 2. The length $L_m(k)$ is calculated for each of the constructed time series S_m^k.

$$L_m(k) = \left[\left(\sum_{i=1}^{\text{int}\,(N-m/k)} |S(m+i.k) - S(m+(i-1).k|). \frac{N-1}{\text{int}\,(N-m/k).k} \right) \right].\text{k}^{-1}. \tag{10}$$

Here the curve length is given by $L_m(k)$ and $(N-1) * (\text{int}\,(N-m/k).\text{k})^{-1}$ is the normalization factor.

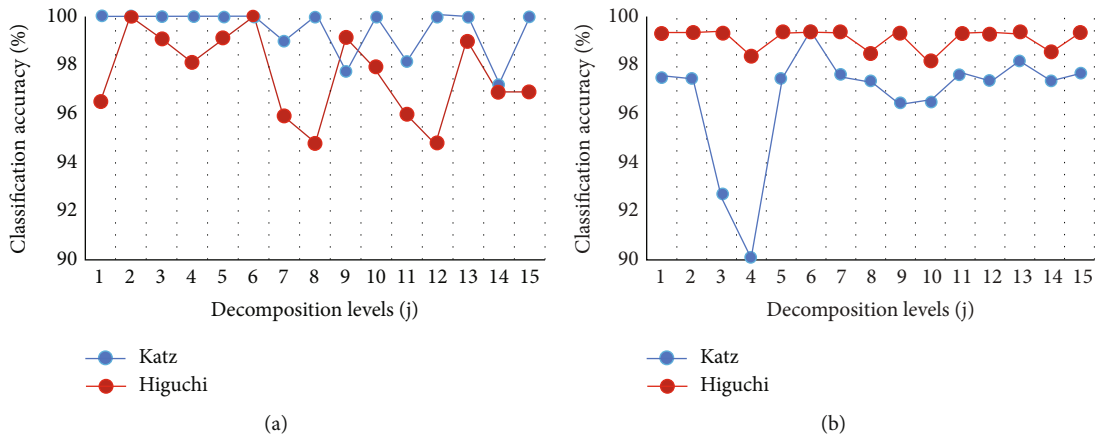

FIGURE 5: Classification accuracy for different decomposition levels for EEG signals under (a) eyes-closed state (b) eyes-open state.

Stage 3. The average length $L_{avg}(k)$ of the curve is calculated by the following equation for each interval of k:

$$L_{\text{avg}}(k) = \frac{1}{k}\sum_{m=1}^{k} L_m(k) \tag{11}$$

For all values of k ranging from 1 to $k_{\max}$, average length calculation is repeated.

Stage 4. The length of the total average curve, $L_{avg}(k)$ is proportional to k^{-D}, where D is the Higuchi fractal dimension (HFD). The slope of the least-squares linear best fit is the estimation of the fractal dimension in the curve of $\ln(L_{avg}(k))$ versus $\ln(1/k)$ in the curve [52]. The parameter time interval k determined the HFD value. In this analysis, we employed k in a certain range of values, which resulted in a specific HFD value.

2.3.2. Katz's Fractal Dimension. In the Katz fractional dimension method [54], the ratio of the curve's total length to the line for the maximum Euclidean distance from the starting point line. In general, the planar curve's fractal dimension, FD_{katz}, is determined by the given equation,

$$\text{FD}_{\text{katz}} = \frac{\log(L)}{\log(d)}, \tag{12}$$

where L denotes the overall length of the curve, or the sum of distances between successive points, and d denotes the diameter, which is calculated as the distance between the first and farthest point on the sequence and given as,

$$L = \sum_{i=1}^{N} \|w_{i+1} - w_i\|, \tag{13}$$

$$d = \max \|w_i - w_1\|. \tag{14}$$

Here, the Euclidean distance is denoted by "$\|.\|$". The fractal dimension (FD) compares the number of units that make up a curve to the smallest number of units required to generate a structure with the same spatial area. The measurement units used to compute FDs have an impact on the results. The average step or average distance between successive points, "a" is created as a general unit or yardstick in Katz's approach [50, 55]. According to Katz's approach, the fractal dimension (FD_{katz}), is expressed as:

$$\text{FD}_{\text{katz}} = \frac{\log(L/a)}{\log(d/a)} = \frac{\log(N)}{\log(d/L) + \log(N)} \tag{15}$$

where, Katz proposed normalize L is the length of the middle stage and d is the average distance between successive points $a = L/N$, where N is the number of steps in the curve.

3. Results and Discussions

The tunable Q-factor wavelet transform approach is used to extract unique features from all 16 channels of EEG signals. EEG data from ADHD and normal subjects are decomposed into multiple levels, and Higuchi and Katz's fractal dimensional features are obtained. The total extracted features for each fractal measures are 112 since six level wavelet decompositions have been performed using TQWT. Hence, a total of 7 wavelet coefficients with respect to 16 EEG channels ($16^*7 = 112$) the size of the features that have been taken. For improved classification accuracy, the optimal selection of quality factor (Q) and decomposition levels (j) is investigated. The redundancy (r) value is fixed to 3 in order to perform better [42, 51]. The TQWT technique is applied on the EEG signals of both ADHD and normal subjects under eyes-closed and eyes-open states for extracting different subbands for different Q and j values. Initially, keeping the Q as 1 and the features are extracted for all the 15 decomposition levels. The unique features extracted with Higuchi and Katz fractional dimension decomposition methods are fed into different classifiers for investigating the efficiency in terms of classification accuracy. Classifiers such as linear discriminant, logistic regression, support vector machine, k-nearest neighbour, ensemble and artificial neural networks are experimented. In all of the experimental conditions, decomposition level 6 achieved maximum classification accuracy. After setting the j value to 6, the Q value is changed from 1 to 10, and the Katz and Higuchi features are computed

for each of the 6 + 1 (7) subbands including one low pass subband are considered. The total number of samples examined in this study is 6400, with 25 second EEG data sets collected. The classification accuracy of each classifier for the EEG signals under the eyes-open state and eyes-closed state are demonstrated in Figure 4.

On observing the classification accuracies of different classifiers, the ANN classifier has exhibited the highest classification accuracy among all the classifiers in both eyes-closed and eyes-open states EEG analysis. Because the ANN classifier outperformed all other classifiers in terms of classification accuracy, only the ANN classifier is used for further investigation. The results are analysed under eyes-open state and eyes-closed for both ADHD and normal subjects. The potential features extracted from all the 15 decomposed levels of EEG signal under eyes-closed and eyes-open states. Figure 5 demonstrates the classification accuracy of both feature extraction methods under eyes-closed and eyes-open states, respectively, for different decomposition levels. It is evident that the potential features extracted from the Katz have maximum classification accuracy in a greater number of decomposition levels than the Higuchi under eyes-closed state. In the meantime, the Higuchi fractional dimension could provide more features that can reflect ADHD in more decomposition levels under the eyes-open state.

In order to determine the best Q and j values, a series of experiments are carried out. While keeping the quality factor $Q = 1$ and redundancy factor $r = 3$ as constants and extracting the unique features from Katz and Higuchi fractal dimensions for all the 15 decomposition levels, it exhibits that the classification accuracy reaches its maximum significant in the 6^{th} level in both the feature extraction methods under eyes-closed and eyes-open states. After choosing $j = 6$ as the decomposition level, the quality factor is changed from 1 to 10, and the characteristics extracted from all 7 subbands $(j + 1)$ for each value of Q are compared. Unique features extracted using Higuchi fractal dimension and Katz's fractal dimension techniques are distinct for ADHD and normal subjects EEG signals. An artificial neural network classifier with a 10-fold cross-validation method is used to validate the classified results. The classification accuracy at different Q values while keeping the decomposition levels 6 as constant is shown in Table 1(b).

The feature extraction techniques used are Katz and Higuchi for both eyes-closed and eyes-open condition. For each technique, 112 features are extracted and given to the ANN classifier. The classification accuracy obtained are shown in the Tables 1–3 for different levels 3, 6, and 8 with Q-factor varying from 1 to 10. Among these, level 6 is giving the best accuracy. The features extracted through Katz fractional dimension have a higher potential to discriminate the ADHD and normal subjects under an eyes-closed state. The EEG signals with eyes-closed states are more significant with higher classification accuracy than the eyes-open state in ADHD diagnosis using Katz fractional dimension estimation method. The classification accuracy became maximum at the decomposition level 6 consistently at $Q = 1$ for both feature extraction methods indicating that the filter banks are perfectly tuned to the optimal classification accuracy at the 6^{th} decomposition level.

Table 1: (a) Classification accuracy for different Q values for a fixed decomposition level $j = 3$, (b) Classification accuracy for different Q values for a fixed decomposition level $j = 6$, (c) Classification accuracy for different Q values for a fixed decomposition level $j = 8$

(a)

Level = 3	Eyes-closed		Eyes-open	
Q	Katz	Higuchi	Katz	Higuchi
1	99.17	91.67	99.00	99.00
2	98.75	95.92	87.42	98.75
3	95.92	93.17	91.67	91.67
4	95.92	69.33	84.08	87.42
5	99.17	70.00	88.17	95.92
6	99.17	82.50	84.08	99.17
7	99.17	84.08	91.67	99.17
8	99.17	88.83	84.08	95.92
9	99.17	87.42	88.17	98.75
10	99.17	88.17	98.75	95.92

(b)

Level = 6	Eyes-closed		Eyes-open	
Q	Katz	Higuchi	Katz	Higuchi
1	100.00	94.25	100.00	100.00
2	99.17	98.75	88.17	99.00
3	98.17	95.92	92.92	92.67
4	98.17	70.00	87.83	89.00
5	100.00	69.33	91.67	97.17
6	100.00	84.08	86.50	100.00
7	100.00	82.50	93.17	100.00
8	100.00	87.42	86.58	97.17
9	100.00	88.83	92.00	99.17
10	100.00	78.25	93.83	97.75

(c)

Level = 8	Eyes-closed		Eyes-open	
Q	Katz	Higuchi	Katz	Higuchi
1	99.17	91.67	99.17	99.17
2	98.75	95.92	84.08	98.75
3	98.75	91.67	90.67	90.17
4	98.75	69.33	86.50	88.17
5	99.00	68.17	90.17	95.92
6	99.00	82.50	86.50	99.17
7	99.00	84.50	91.67	99.17
8	99.00	86.50	86.50	98.75
9	99.00	84.08	89.67	98.75
10	99.00	69.33	91.67	95.92

Table 2: Performance metrics for Katz and Higuchi feature extraction methods (a) eyes-closed state (b) eyes-open state.

(a)

Level = 6	Accuracy		Sensitivity		NPV		MCC		F1-score		G-mean	
Q	Katz	Higuchi	Katz	Higuchi	Katz	Higuchi	Katz	Higuchi	Katz	Higuchi	Katz	Higuchi
1	100	94.25	100	89.17	100	91.3	100	90.16	100	93.33	100	93.95
2	99.2	98.75	98.33	97.5	98.75	98.3	98.54	97.89	99	98.33	99.08	98.54
3	98.2	95.92	95.83	91.67	97.5	94.2	96.6	92.82	97.33	94.67	97.62	95.24
4	98.2	70	95.83	66.67	97.5	65	96.6	41.37	97.33	69.52	97.62	65.13
5	100	69.33	100	58.33	100	66.7	100	43.46	100	65.17	100	67.23
6	100	84.08	100	76.67	100	80.4	100	70.52	100	82	100	83.39
7	100	82.5	100	75.83	100	80.4	100	67.56	100	80.17	100	81.7
8	100	87.42	100	80.83	100	84.6	100	76.4	100	85.67	100	86.75
9	100	88.83	100	86.67	100	90.8	100	78.97	100	87.24	100	87.16
10	100	78.25	100	73.33	100	77.1	100	58.79	100	76.5	100	76.99

(b)

Level = 6	Accuracy		Sensitivity		NPV		MCC		F1-score		G-mean	
Q	Katz	Higuchi	Katz	Higuchi	Katz	Higuchi	Katz	Higuchi	Katz	Higuchi	Katz	Higuchi
1	100	100	100	100	100	100	100	100	100	100	100	100
2	88.2	99	76.67	97.5	83.33	98.75	79.8	98.06	85	98.33	86.63	98.54
3	92.9	92.67	87.5	89.17	89.58	92.92	88.46	87.1	91.83	91	92.75	91.39
4	87.8	89	75.83	82.5	83	87.17	79.12	81	84.17	86.79	85.98	87.44
5	91.7	97.17	84.17	95.83	88.33	97.5	86.08	94.66	89.5	96.62	90.74	96.15
6	86.5	100	72.5	100	80.83	100	76.34	100	82.33	100	84.24	100
7	93.2	100	86.67	100	90.42	100	88.37	100	91.17	100	92.21	100
8	86.6	97.17	73.33	100	81.33	100	77	95.2	82.5	97.29	84.51	97.25
9	92	99.17	84.17	100	88.33	100	86.11	98.54	90	99.29	91.02	99.08
10	93.8	97.75	88.33	100	90.83	100	89.51	96.22	92.67	98	93.4	97.62

3.1. Performance Metrics. The classifier's performance was measured using accuracy, sensitivity, specificity, negative predictive value (NPV) and positive predictive value (PPV), F1-score, G-mean, and Matthew's correlation coefficient (MCC). The mathematical background of each performance metric is given as follows:

The percentage of true positives (TP) and true negatives (TN) over the total number of true positive (TP), true negative (TN), false positive (FP), and false negative (FN) individuals was used to calculate the classification performance for accuracy.

$$\text{Accuracy}\,(\%) = \frac{(\text{TP} + \text{TN})}{(\text{TP} + \text{TN} + \text{FP} + \text{FN})} * 100 \tag{16}$$

Sensitivity is calculated by dividing the number of true positive (TP) cases by the number of genuine positive cases, i.e., the total of true positive (TP) and false negative (FN) cases.

$$\text{Sensitivity}\,(\%) = \frac{\text{TP}}{(\text{TP} + \text{FN})} * 100 \tag{17}$$

Specificity refers to the number of true negative (TN) cases found among all actual negative cases, i.e., the total of true negative and false positive (FP) cases.

$$\text{Specificity}\,(\%) = \frac{\text{TN}}{(\text{TN} + \text{FP})} * 100 \tag{18}$$

The ratio of true positives to the number of positive brain maps is known as the positive predictive value (PPV).

$$\text{Positive Predictive Value}(\%) = \frac{\text{TP}}{(\text{TP} + \text{FP})} * 100 \tag{19}$$

The ratio of true negative to the number of negative brain maps defines the negative predictive value (NPV).

$$\text{Negative Predictive Value}(\%) = \frac{\text{TN}}{(\text{TN} + \text{FN})} * 100 \tag{20}$$

Table 3: Summary of comparison for automated detection of ADHD with state-of-the-art techniques.

S.no	Authors	Year	Participants	Age group	Feature extraction methodology	Classifiers	Classification accuracy (%)
1	Ghaderyan et al. [56]	2022	14 ADHD and 19 healthy children	6 to 11 years	Dynamic frequency wrapping	Sparse nonnegative least-square coding	99.17%
2	Tor et al. [34]	2021	45 ADHD, 62 (ADHD+CD) and 16 CD	6 to 12 years	Nonlinear features	KNN classifier	97.88%
3	Ahmadi et al. [35]	2021	13 ADHD-C subtype, 12 ADHD-I subtype, 14 control	6 to 11 years old	Spatial and frequency band features	Convolutional neural network	99.46%
4	R et al. [25]	2021	5 ADHD and 5 normal subjects with eyes-open and eyes-closed state	7 to 12 years	Permutation entropy, Sure entropy, log energy entropy, fuzzy entropy	ANN classifier	99.82%
5	Ekhlasi et al. [36]	2021	61 ADHD and 60 healthy children	9.62 is the mean age of ADHD, 9.85 is the mean age of control group	Directed phase transfer entropy	ANN classifier	89.1%
6	Moghaddari et al. [37]	2020	31 ADHD and 30 healthy children	7 to 12 years	Frequency band separation	Deep CNN	98.48%%
7	Rezaeezadeh et al. [57]	2020	12 ADHD and 12 normal subjects with eyes-closed condition	7–12 years old	Nonlinear and linear univariate features	SVM, KNN, PNN	99.58%
8	Dubreuil-Vall et al. [58]	2020	20 healthy and 20 ADHD patients		Features extracted from neural network	CNN, RNN, SNN	88%
9	Kaur et al.[59]	2020	47 ADHD and 50 control during the eyes-open, eyes-closed, and continuous performance test (CPT) condition	20.3 is the mean age of ADHD, 20.6 is the mean age of normal	Phase space reconstruction, statistical features	SVM, KNN, neural dynamic classifier, enhanced probabilistic neural network, and naive-Bayes classifier	93.3%
10	Altınkaynak et al. [60]	2020	23 ADHD and 23 healthy controls	7–12 years	Morphological, wavelets, and nonlinear based features	Multilayer perceptron, Naïve Bayes, support vector machines, k-nearest neighbor, adaptive boosting, logistic regression and random forest	91.3%
11	Chang et al. [61]	2019	100 ADHD, 44 Normal subjects	10.9 ± 2.4, 10.6 ± 1.9 mean age of ADHD, 11.3 ± 2.2 mean age of normal	Time points, channels input features, saliency maps	Deep EEGNet	83%
12	Boroujeni et al. [29]	2019	50 ADHD and 26 normal cases	4 to 15 years old	Lyapunov exponent, fractal dimension, correlation dimension and sample, fuzzy and approximate entropies	SVM classifier	96.05%

Table 3: Continued.

S.no	Authors	Year	Participants	Age group	Feature extraction methodology	Classifiers	Classification accuracy (%)
13	Chang et al. [61]	2019	30 ADHD and 30 control subjects	Mean age in the ADHD group was 8 years 5 months ±1 year 11 months, control group was 8 years 5 months ±1 year 8 months	Univariate and multivariate features	SVM classifier	Area under the curve = 87.78%, sensitivity = 80.0%, specificity = 80.0%
14	Bashiri et al. [62]	2018	95 ADHD subjects	7 to 18 years old	QEEG features, integrated visual and auditory continuous performance test	ANN classifier	To determine the existence or absence of attention and response control in ADHD subjects
15	Khoshnoud et al. [23]	2018	12 ADHD and 12 normal children	7–12 years old	Frequency band powers, nonlinear features	SVM classifier	83.33%
16	Karimu et al. [28]	2018	20 ADHD and 20 normal children	7–10 years.	Mixture of expert fuzzy models	Continuous wavelet transform (CWT) and standalone classifier	98.01%
17	Chow et al. [63]	2018	30 ADHD and 30 controls.	Mean age for control group 7 years and 10 months ±2 years and 2 months, mean age for ADHD 8 years and 1 month ±2 years	ApEn and TBR	Logistic regression	81.7%
18	Mohammadi et al. [27]	2016	30 ADHD and 30 healthy children	9.62 ± 1.75 years for ADHD, 9.85 ± 1.77 years for healthy children	Fractal dimension (FD), approximate entropy and Lyapunov exponent	Multilayer perceptron	93.65%
19	Khoshnoud et al. [64]	2016	12 ADHD and 10 control groups	8-13 years old	Largest Lyapunov exponent and approximate entropy	Probabilistic neural network classifier	87.5%
20	Helgadóttir et al. [65]	2015	310 ADHD and 351 controls	5.8 to 14 years	Spectral features extraction	Multivariate diagnostic classifier	76%
21	Tenev et al. [8]	2014	67 ADHD, 50 controls	18 to 50 years of age	Forward selection for feature extraction	SVM classifier	82.3%
22	González et al. [66]	2013	22 ADHD and 21 healthy controls	4–15 years	Multivariate linear and nonlinear interdependence measures	Logistic regression	86.7%
23	Nazhvani et al. [67]	2013	12 healthy ones, 12 with ADHD and 12 with BMD	10 to 22 years old	Wavelet denoising and synchronous averaging features	KNN classifier	92.85%
24	Abibullaev et al. [68]	2012	7 ADHD and 3 normal groups	7–12 years	Shanon's entropy, mutual information measures	SVM classifier	97%
25	Ahmadlou and Adeli [40]	2011	12 ADHD and 12 control participants	8–13 years old	Fuzzy synchronization likelihood	Leave one out cross-validation method	87.50%

Table 3: Continued.

S.no	Authors	Year	Participants	Age group	Feature extraction methodology	Classifiers	Classification accuracy (%)
26	Ahmadlou and Adeli [38]	2010	47 ADHD and 7 control individuals with eyes-closed	7-12 years old	Wavelet decomposition and synchronization likelihood method.	RBF neural network classifier	95.6%
27	Proposed work	2022	5 ADHD and 5 non-ADHD subjects with eyes-open and eyes-closed state	6-12 years old	Tunable Q-factor wavelet transform	Linear discriminant, logistic regression, support vector machine, artificial neural networks, and ensemble	100%

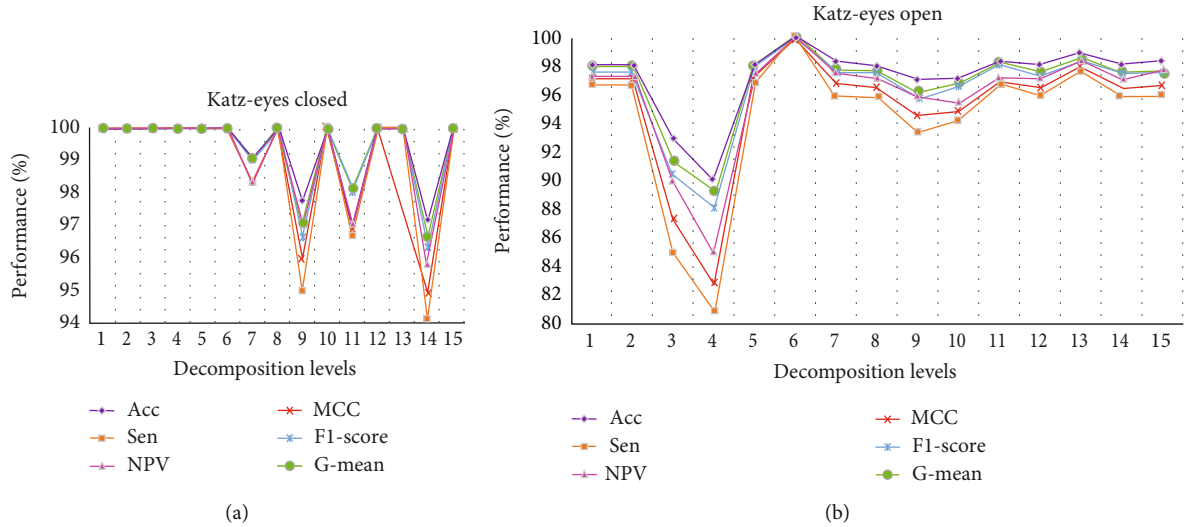

FIGURE 6: Performance analysis of Katz fractional dimension with different decomposition levels (a) eyes-closed state (b) eyes-open states.

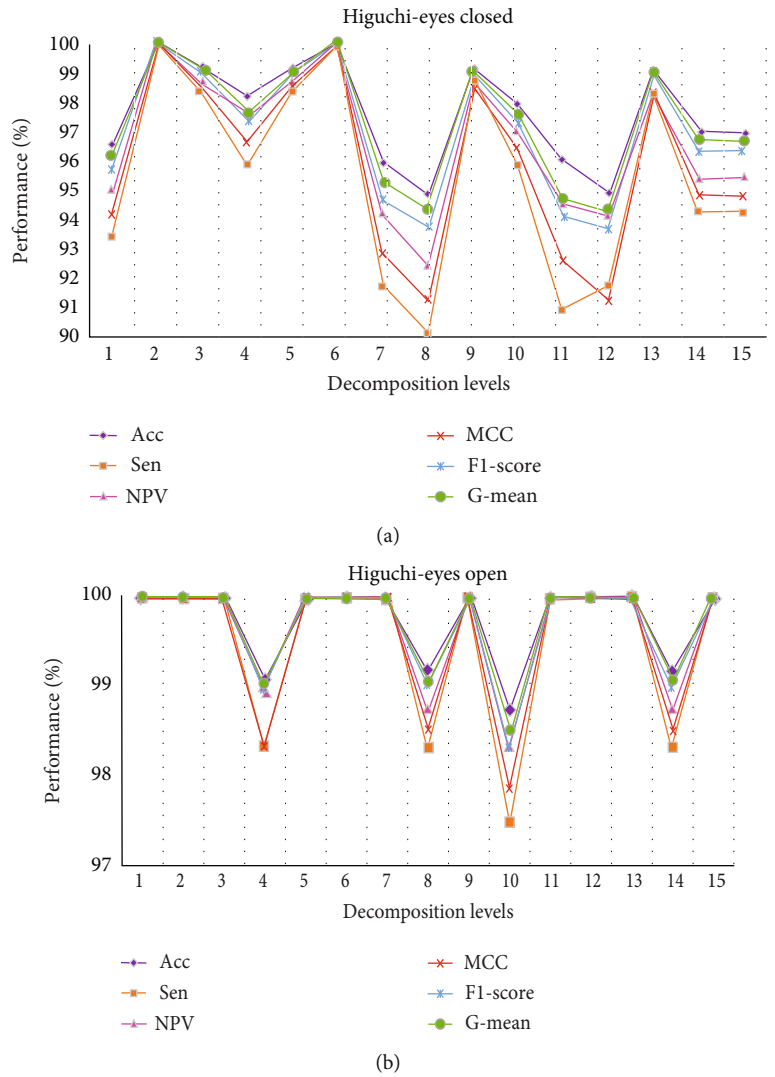

FIGURE 7: Performance analysis of Higuchi fractional dimension with different decomposition levels (a) eyes-closed state (b) eyes-open states.

The harmonic and geometric measurements of sensitivity and specificity are the F1-score and G-mean, respectively.

$$\text{F1} - \text{Score}\,(\%) = \frac{(2 * \text{Sensiitivity} * \text{PPV})}{(\text{Sensiitivity} + \text{PPV})} * 100 \quad (21)$$

$$\text{G}_{\text{mean}}\,(\%) = \sqrt{\text{Sensitivity} * \text{Specificity}} * 100 \quad (22)$$

Matthew's correlation coefficient is a balanced metric that determines both true and false positives and negatives, even if the classes are of different sizes [55]. To determine a result, the MCC takes into account the test's true positives (TP), true negatives (TN), false positives (FP), and false negatives (FN), and a significant prediction is one. Matthew's correlation coefficient (MCC) is calculated as:

$$\text{MCC} = \frac{(\text{TP} * \text{TN}) - (\text{FP} * \text{FN})}{\sqrt{(\text{TP} + \text{FP})(\text{TP} + \text{FN})(\text{TN} + \text{FN})}} * 100 \quad (23)$$

The classification process for ADHD and normal subjects under eyes-closed and eyes-open conditions with different decomposition levels j varying from 1 to 15 is performed. The above performance metrics are evaluated and plotted against the decomposition levels which is shown in Figures 6 and 7. While comparing the performances in the Katz fractional dimension method, the eyes-closed state shown in Figure 6(a) reflects that the classification accuracy, sensitivity, and all other performance matrices are consistently stable at 100% in the lower decomposition level up to level 6 and the variation observed in higher levels of decomposition. This indicates that significant features are extracted in the eyes-closed state and it has a higher ability of discrimination at lower decomposition levels. In the meantime, the EEG signals with eyes-open states shown in Figure 6(b) indicate that the performance metrices has a lesser value at lower decomposition levels, and improve at higher decomposition levels. It reflects that the potential features to discriminate the ADHD are more significant and the ability of the classifier is increased in higher decomposition levels.

Table 2 presents the statistical details of different performance matrices while keeping the decomposition level 6 as constant and varying the tuning factor Q. The filter banks are tuned for its best performance at decomposition level 6, and observed that the Katz feature extraction method showed higher significance in classifying the ADHD under eyes-closed state with higher classification accuracy and sensitivity. Meanwhile, the Higuchi feature extraction method showed higher performance with higher classification accuracy and sensitivity under eyes-open state.

The classification accuracy of the proposed work is compared with the similar works of various authors and observed an improvement in performance. Table 3 shows the performance comparison specifically in terms of classification accuracy. The proposed methodology exhibits the maximum performance with 100% classification accuracy.

It is clear, classify, and diagnose attention deficit hyperactive disorder from the EEG signals has been used many techniques and applications such as ANN, Fog computing, Internet of Medical Thing, and other methods [69–74].

The merit of the proposed methodology is that it has given the highest classification accuracy and this is a robust system as it is validated with 10 fold cross-validation for different classifiers. The limitation of the present work is that it needs preprocessed artifact-free EEG signals, that add an additional signal processing stage to the implementation of the proposed method for real-time diagnostic purposes. Also, the data set shall be extended to fine-tune the system performances in analysing the effectiveness of the proposed system.

4. Conclusion

The present work is an effective methodology to classify and diagnose attention deficit hyperactive disorder from the EEG signals. The EEG signals of both ADHD and normal subjects recorded under eyes-closed and eyes-open states are preprocessed and the tunable Q-wavelet transform is applied to decompose into different subbands. The Katz and Higuchi fractional dimension feature extraction techniques are applied to extract the features for the effective classification of ADHD and normal subjects with the possible maximum accuracy. The Q-value and the decomposition levels are optimally tuned to extract the potential features that can bring out the maximum classification accuracy. Different classifiers have experimented and the artificial neural network classifier with a 10-fold cross-validation method is found to be an effective classifier with a maximum classification accuracy of 100%. According to the findings, the level of decomposition and the Q-factor parameter has a significant impact on feature extraction performance. The classification accuracy varies dramatically with different Q-factor values, with decomposition level j of 6 being the most appropriate. Moreover, the Katz fractional dimension algorithm shows better results in eyes-closed states and the Higuchi FD algorithm demonstrates better results under eyes-open states. Different performance metrics are used to measure the effectiveness of the classifier algorithm that has justified the observed results. The features extracted through Katz and Higuchi from EEG signal under the eyes-closed state in lower decomposition levels have higher significance in discriminating ADHD from the normal subjects. Also, the features extracted from the eyes-open state in higher decomposition levels have higher significance in estimating ADHD with higher classification accuracy. With the eyes-closed EEG signals, the Katz feature extraction method showed greater significance with higher sensitivity in diagnosing ADHD. Meanwhile, the Higuchi feature extraction method showed higher performance with higher sensitivity under eyes-open state signals. As the proposed system has given the highest classification accuracy with higher sensitivity, this shall be used in the clinical diagnosis of ADHD.

Data Availability

The data sets are not publicly available. The data used to support the findings of this study are available from the corresponding author upon request.

Conflicts of Interest

The authors declare that there is no conflict of interest.

References

[1] K. Konrad and S. B. Eickhoff, "Is the ADHD brain wired differently? A review on structural and functional connectivity in attention deficit hyperactivity disorder," *Human Brain Mapping*, vol. 31, no. 6, pp. 904–916, 2010.

[2] E. Cormier, "Attention seficit/hyperactivity disorder: a review and update," *Journal of Pediatric Nursing*, vol. 23, no. 5, pp. 345–357, 2008.

[3] M. Smith, "Hyperactive around the world? The history of ADHD in global perspective," *Social History of Medicine*, vol. 30, no. 4, pp. 767–787, 2017.

[4] J. A. Venkata and A. S. Panicker, "Prevalence of attention deficit hyperactivity disorder in primary school children," *Indian Journal of Psychiatry*, vol. 55, no. 4, pp. 338–342, 2013.

[5] J. Monge, C. Gómez, J. Poza, A. Fernández, J. Quintero, and R. Hornero, "MEG analysis of neural dynamics in attention-deficit/hyperactivity disorder with fuzzy entropy," *Medical Engineering & Physics*, vol. 37, no. 4, pp. 416–423, 2015.

[6] A. R. Clarke, R. J. Barry, R. Mccarthy, and M. Selikowitz, "EEG-defined subtypes of children with attention-deficit / hyperactivity disorder," vol. 112, pp. 2098–2105, 2001, http://www.elsevier.com/locate/clinph.

[7] M. Arns, H. Heinrich, and U. Strehl, "Evaluation of neurofeedback in ADHD: the long and winding road," *Biological Psychology*, vol. 95, no. 1, pp. 108–115, 2014.

[8] A. Tenev, S. Markovska-Simoska, L. Kocarev, J. Pop-Jordanov, A. Müller, and G. Candrian, "Machine learning approach for classification of ADHD adults," *International Journal of Psychophysiology*, vol. 93, no. 1, pp. 162–166, 2014.

[9] L. Bergeron, J. P. Valla, J. J. Breton et al., "Correlates of mental disorders in the Quebec general population of 6 to 14-year olds," *Journal of Abnormal Child Psychology*, vol. 28, no. 1, pp. 47–62, 2000.

[10] E. J. Costello, D. L. Foley, and A. Angold, "10-year research update review: the epidemiology of child and adolescent psychiatric disorders: II. developmental epidemiology," *Journal of the American Academy of Child and Adolescent Psychiatry*, vol. 45, no. 1, pp. 8–25, 2006.

[11] E. Emerson, S. Einfeld, and R. J. Stancliffe, "The mental health of young children with intellectual disabilities or borderline intellectual functioning," *Social Psychiatry and Psychiatric Epidemiology*, vol. 45, no. 5, pp. 579–587, 2010.

[12] S. Patidar, R. B. Pachori, A. Upadhyay, and U. Rajendra Acharya, "An integrated alcoholic index using tunable- Q wavelet transform based features extracted from EEG signals for diagnosis of alcoholism," *Applied Soft Computing*, vol. 50, pp. 71–78, 2017.

[13] J. P. Amezquita-sanchez, N. Mammone, F. C. Morabito, and H. Adeli, "A New dispersion entropy and fuzzy logic system methodology for automated classification of dementia stages using electroencephalograms," *Clinical Neurology and Neurosurgery*, vol. 201, p. 106446, 2021.

[14] P. Durongbhan, Y. Zhao, L. Chen et al., "A dementia classification framework using frequency and time-frequency features based on EEG signals," *IEEE Transactions on Neural Systems and Rehabilitation Engineering*, vol. 27, no. 5, pp. 826–835, 2019.

[15] A. Bhattacharyya, L. Singh, and R. B. Pachori, "Identification of epileptic seizures from scalp EEG signals based on TQWT," *Advances in Intelligent Systems and Computing*, vol. 748, pp. 209–221, 2019.

[16] R. Satpathy, T. Choudhury, S. Satpathy, S. N. Mohanty, and X. Zhang, *Data Analytics in Bioinformatics: A Machine Learning Perspective*, John Wiley & Sons, 2021.

[17] A. Sharma, J. K. Rai, and R. P. Tewari, "Schizophrenia detection using biomarkers from electroencephalogram signals," *IETE Journal of Research*, vol. 68, no. 4, pp. 3056–3064, 2022.

[18] S. K. Khare, V. Bajaj, and U. R. Acharya, "Detection of Parkinson's disease using automated tunable Q wavelet transform technique with EEG signals," *Biocybernetics and Biomedical Engineering*, vol. 41, no. 2, pp. 679–689, 2021.

[19] S. L. Oh, Y. Hagiwara, U. Raghavendra et al., "A deep learning approach for Parkinson's disease diagnosis from EEG signals," *Neural Computing and Applications*, vol. 32, no. 15, pp. 10927–10933, 2020.

[20] M. Saeedi, A. Saeedi, and A. Maghsoudi, "Major depressive disorder assessment via enhanced k-nearest neighbor method and EEG signals," *Physical and Engineering Sciences in Medicine*, vol. 43, no. 3, pp. 1007–1018, 2020.

[21] R. A. Movahed, G. P. Jahromi, S. Shahyad, and G. H. Meftahi, "A major depressive disorder classification framework based on EEG signals using statistical , spectral , wavelet , functional connectivity , and nonlinear analysis," *Journal of Neuroscience Methods*, vol. 358, p. 109209, 2021.

[22] G. Alba, E. Pereda, S. Mañas, L. D. Méndez, A. González, and J. J. González, "Electroencephalography signatures of attention-deficit/hyperactivity disorder: clinical utility," *Neuropsychiatric Disease and Treatment*, vol. 11, pp. 2755–2769, 2015.

[23] S. Khoshnoud, M. A. Nazari, and M. Shamsi, "Functional brain dynamic analysis of ADHD and control children using nonlinear dynamical features of EEG signals," *Journal of Integrative Neuroscience*, vol. 17, no. 1, pp. 17–30, 2018.

[24] S. K. Loo and S. Makeig, "Clinical utility of EEG in attention-deficit/hyperactivity disorder: a research update," *Neurotherapeutics*, vol. 9, no. 3, 2012.

[25] R. Catherine Joy, S. Thomas George, A. Albert Rajan, and M. S. P. S. P. Subathra, "Detection of ADHD from EEG signals using different entropy measures and ANN," *Clinical EEG and Neuroscience*, vol. 53, no. 1, 2021.

[26] F. Ghassemi, M. Hassan, M. Tehrani-Doost, and V. Abootalebi, "Using non-linear features of EEG for ADHD/normal participants' classification," *Procedia Social and Behavioral Sciences*, vol. 32, pp. 148–152, 2012.

[27] M. R. Mohammadi, A. Khaleghi, A. M. Nasrabadi, S. Rafieivand, M. Begol, and H. Zarafshan, "EEG classification of ADHD and normal children using non-linear features and neural network," *Biomedical Engineering Letters*, vol. 6, no. 2, pp. 66–73, 2016.

[28] R. Yaghoobi Karimu and S. Azadi, "Diagnosing the ADHD using a mixture of expert fuzzy models," *International Journal of Fuzzy Systems*, vol. 20, no. 4, pp. 1282–1296, 2018.

[29] Y. K. Boroujeni, A. A. Rastegari, and H. Khodadadi, "Diagnosis of attention deficit hyperactivity disorder using non-linear analysis of the EEG signal," *IET Systems Biology*, vol. 13, no. 5, pp. 260–266, 2019.

[30] A. Mueller, G. Candrian, V. A. Grane, J. D. Kropotov, V. A. Ponomarev, and G. M. Baschera, "Discriminating between ADHD adults and controls using independent ERP components

and a support vector machine: a validation study," *Nonlinear Biomedical Physics*, vol. 5, no. 1, pp. 1–18, 2011.

[31] K. Sadatnezhad, R. Boostani, and A. Ghanizadeh, "Classification of BMD and ADHD patients using their EEG signals," *Expert Systems with Applications*, vol. 38, no. 3, pp. 1956–1963, 2011.

[32] O. Article, A. Allahverdy, A. K. Moghaddam, M. R. Mohammadi, and A. M. Nasrabadi, "Detecting ADHD children using the attention continuity as nonlinear feature of EEG," *Frontiers in Biomedical Technologies*, vol. 3, no. 1-5, pp. 28–33, 2016.

[33] E. Pereda, M. García-Torres, B. Melián-Batista, S. Mañas, L. Méndez, and J. J. González, "The blessing of dimensionality: feature selection outperforms functional connectivity-based feature transformation to classify ADHD subjects from EEG patterns of phase synchronisation," *PLoS One*, vol. 13, no. 8, pp. 1–24, 2018.

[34] H. T. Tor, C. P. Ooi, N. S. Lim-Ashworth et al., "Automated detection of conduct disorder and attention deficit hyperactivity disorder using decomposition and nonlinear techniques with EEG signals," *Computer Methods and Programs in Biomedicine*, vol. 200, 2021.

[35] A. Ahmadi, M. Kashefi, H. Shahrokhi, and M. A. Nazari, "Computer aided diagnosis system using deep convolutional neural networks for ADHD subtypes," *Biomedical Signal Processing and Control*, vol. 63, 2021.

[36] A. Ekhlasi, A. M. Nasrabadi, M. Mohammadi, A. Motie Nasrabadi, and M. Mohammadi, "Classification of the children with ADHD and healthy children based on the directed phase transfer entropy of EEG signals," *Frontiers in Biomedical Technologies*, vol. 8, no. 2, pp. 115–122, 2021.

[37] M. Moghaddari, M. Z. Lighvan, and S. Danishvar, "Diagnose ADHD disorder in children using convolutional neural network based on continuous mental task EEG," *Computer Methods and Programs in Biomedicine*, vol. 197, 2020.

[38] M. Ahmadlou and H. Adeli, "Wavelet-synchronization methodology: a new approach for EEG-based diagnosis of ADHD," *Clinical EEG and Neuroscience*, vol. 41, no. 1, pp. 1–10, 2010.

[39] A. Allahverdy, A. M. Nasrabadi, and M. R. Mohammadi, "Detecting ADHD children using symbolic dynamic of nonlinear features of EEG," 2022 https://ieeexplore.ieee.org/abstract/document/5955548.

[40] M. Ahmadlou and H. Adeli, "Functional community analysis of brain: a new approach for EEG-based investigation of the brain pathology," *NeuroImage*, vol. 58, no. 2, pp. 401–408, 2011.

[41] D. P. Dash and M. H. Kolekar, "Hidden Markov model based epileptic seizure detection using tunable Q wavelet transform," *Journal of Biomedical Research*, vol. 34, no. 3, pp. 170–179, 2020.

[42] I. W. Selesnick, "Wavelet transform with tunable Q-factor," *IEEE Transactions on Signal Processing*, vol. 59, no. 8, pp. 3560–3575, 2011.

[43] A. Bhattacharyya, R. B. Pachori, A. Upadhyay, and U. R. Acharya, "Tunable-Q wavelet transform based multiscale entropy measure for automated classification of epileptic EEG signals," *Applied Sciences*, vol. 7, no. 4, 2017.

[44] S. T. George, M. S. P. Subathra, N. J. Sairamya, L. Susmitha, and M. Joel Premkumar, "Classification of epileptic EEG signals using PSO based artificial neural network and tunable-Q wavelet transform," *Biocybernetics and Biomedical Engineering*, vol. 40, no. 2, pp. 709–728, 2020.

[45] W. He, Y. Zi, B. Chen, F. Wu, and Z. He, "Automatic fault feature extraction of mechanical anomaly on induction motor bearing using ensemble super-wavelet transform," *Mechanical Systems and Signal Processing*, vol. 54, pp. 457–480, 2015.

[46] M. Murugappan, W. Alshuaib, A. K. Bourisly, S. K. Khare, S. Sruthi, and V. Bajaj, "Tunable Q wavelet transform based emotion classification in Parkinson's disease using electroencephalography," *PLoS One*, vol. 15, no. 11, 2020.

[47] V. Bajaj, S. Taran, S. K. Khare, and A. Sengur, "Feature extraction method for classification of alertness and drowsiness states EEG signals," *Applied Acoustics*, vol. 163, 2020.

[48] A. R. Hassan, S. Siuly, and Y. Zhang, "Epileptic seizure detection in EEG signals using tunable-Q factor wavelet transform and bootstrap aggregating," *Computer Methods and Programs in Biomedicine*, vol. 137, pp. 247–259, 2016.

[49] S. K. Khare and V. Bajaj, "Constrained based tunable Q wavelet transform for efficient decomposition of EEG signals," *Applied Acoustics*, vol. 163, 2020.

[50] R. Acharya, O. Faust, N. Kannathal, T. Chua, and S. Laxminarayan, "Non-linear analysis of EEG signals at various sleep stages," *Computer Methods and Programs in Biomedicine*, vol. 80, no. 1, pp. 37–45, 2005.

[51] K. Jindal, R. Upadhyay, and H. S. Singh, "Application of tunable-Q wavelet transform based nonlinear features in epileptic seizure detection," *Analog Integrated Circuits and Signal Processing*, vol. 100, no. 2, pp. 437–452, 2019.

[52] A. Rizal and R. D. Estananto, "Epileptic EEG signal classification using multiresolution Higuchi fractal dimension," *International Journal of Engineering Research & Technology*, vol. 12, no. 4, pp. 508–511, 2019, http://www.irphouse.com508.

[53] M. Bachmann, J. Lass, A. Suhhova, and H. Hinrikus, "Spectral asymmetry and Higuchi's fractal dimension measures of depression electroencephalogram," *Computational and Mathematical Methods in Medicine*, vol. 2013, Article ID 251638, 8 pages, 2013.

[54] M. J. Katz, "Fractals and the analysis of waveforms," *Computers in Biology and Medicine*, vol. 18, no. 3, pp. 145–156, 1988.

[55] S. M. Fernandez-Fraga and J. Rangel, "Comparison of Higuchi, Katz and multiresolution box-counting fractal dimension algorithms on EEG waveforms signals based on visual evoked potentials," *Revista EIA/English Version*, vol. 14, no. 27, 2017.

[56] P. Ghaderyan, F. Moghaddam, S. Khoshnoud, and M. Shamsi, "New interdependence feature of EEG signals as a biomarker of timing deficits evaluated in attention-deficit/hyperactivity disorder detection," *Measurement*, vol. 199, 2022.

[57] M. Rezaeezadeh, S. Shamekhi, and M. Shamsi, "Attention deficit hyperactivity disorder diagnosis using non-linear univariate and multivariate EEG measurements: a preliminary study," *Physical and Engineering Sciences in Medicine*, vol. 43, no. 2, pp. 577–592, 2020.

[58] L. Dubreuil-Vall, G. Ruffini, and J. A. Camprodon, "Deep learning convolutional neural networks discriminate adult ADHD from healthy individuals on the basis of event-related spectral EEG," *Frontiers in Neuroscience*, vol. 14, p. 251, 2020.

[59] S. Kaur, S. Singh, P. Arun, D. Kaur, and M. Bajaj, "Phase space reconstruction of EEG signals for classification of ADHD and control adults," *Clinical EEG and Neuroscience*, vol. 51, no. 2, pp. 102–113, 2020.

[60] M. Altınkaynak, N. Dolu, A. Güven et al., "Diagnosis of attention deficit hyperactivity disorder with combined time and frequency features," *Biocybernetics and Biomedical Engineering*, vol. 40, no. 3, pp. 927–937, 2020.

[61] M. Y. Chang, C. S. Ouyang, C. T. Chiang et al., "A new method of diagnosing attention-deficit hyperactivity disorder in male patients by quantitative EEG analysis," *Clinical EEG and Neuroscience*, vol. 50, no. 5, pp. 339–347, 2019.

[62] A. Bashiri, L. Shahmoradi, H. Beigy et al., "Quantitative EEG features selection in the classification of attention and response control in the children and adolescents with attention deficit hyperactivity disorder," *Future Science OA*, vol. 4, no. 5, pp. 11–13, 2018.

[63] J. C. Chow, C. S. Ouyang, C. L. Tsai et al., "Entropy-based quantitative electroencephalogram analysis for diagnosing attention-deficit hyperactivity disorder in girls," *Clinical EEG and Neuroscience*, vol. 50, no. 3, pp. 172–179, 2019.

[64] S. Khoshnoud, M. Shamsi, and M. A. Nazari, "Non-linear EEG analysis in children with attention-deficit/ hyperactivity disorder during the rest condition," in *2015 22nd Iranian Conference on Biomedical Engineering (ICBME)*, Tehran, Iran, 2016.

[65] H. Helgadóttir, Ó. Ó. Gudmundsson, G. Baldursson et al., "Electroencephalography as a clinical tool for diagnosing and monitoring attention deficit hyperactivity disorder: a cross-sectional study," *BMJ Open*, vol. 5, no. 1, 2015.

[66] J. J. González, L. D. Méndez, S. Mañas, M. R. Duque, E. Pereda, and L. De Vera, "Performance analysis of univariate and multivariate EEG measurements in the diagnosis of ADHD," *Clinical Neurophysiology*, vol. 124, no. 6, pp. 1139–1150, 2013.

[67] A. D. Nazhvani, R. Boostani, S. Afrasiabi, and K. Sadatnezhad, "Classification of ADHD and BMD patients using visual evoked potential," *Clinical Neurology and Neurosurgery*, vol. 115, no. 11, pp. 2329–2335, 2013.

[68] B. Abibullaev and J. An, "Decision support algorithm for diagnosis of ADHD using electroencephalograms," *Journal of Medical Systems*, vol. 36, no. 4, pp. 2675–2688, 2012.

[69] T. Y. Wah, M. A. Mohammed, U. Iqbal, S. Kadry, A. Majumdar, and O. Thinnukool, "Novel DERMA fusion technique for ECG heartbeat classification," *Life*, vol. 12, no. 6, p. 842, 2022.

[70] A. A. Mutlag, M. K. Abd Ghani, M. A. Mohammed et al., "Multi-agent systems in fog–cloud computing for critical healthcare task management model (CHTM) used for ECG monitoring," *Sensors*, vol. 21, no. 20, p. 6923, 2021.

[71] A. A. Mutlag, M. K. A. Ghani, and M. A. Mohammed, "A healthcare resource management optimization framework for ECG biomedical sensors," in *In Efficient Data Handling for Massive Internet of Medical Things*, pp. 229–244, Springer, Cham, 2021.

[72] A. U. Rahman, M. Saeed, M. A. Mohammed, M. M. Jaber, and B. Garcia-Zapirain, "A novel fuzzy parameterized fuzzy hypersoft set and Riesz summability approach based decision support system for diagnosis of heart diseases," *Diagnostics*, vol. 12, no. 7, p. 1546, 2022.

[73] J. Prasanna, M. S. P. Subathra, M. A. Mohammed, R. Damaševičius, N. J. Sairamya, and S. T. George, "Automated epileptic seizure detection in pediatric subjects of CHB-MIT EEG database—a survey," *Journal of Personalized Medicine*, vol. 11, no. 10, p. 1028, 2021.

[74] M. S. P. Subathra, M. A. Mohammed, M. S. Maashi, B. Garcia-Zapirain, N. J. Sairamya, and S. T. George, "Detection of focal and non-focal electroencephalogram signals using fast Walsh-Hadamard transform and artificial neural network," *Sensors*, vol. 20, no. 17, p. 4952, 2020.